

# Electrochemical Deposition of Ni-Zn Oxide Coatings on Roll Knife Surfaces: Process Parameters and Performance Effects

Quangang Li, Jianbo Zhou\*, Xiaohong Wang

Harbin Research Institute of Forestry Machinery, National Forestry and Grassland Administration, Harbin 150086, Heilongjiang, China

received June 30, 2025; received in revised form August 4, 2025; accepted September 5, 2025

## Abstract

An innovative electrodeposition method was developed to fabricate Ni-ZnO composite coatings on high-carbon stainless steel substrates for industrial cutting applications. In this study, key deposition parameters including current density (ranging from 2 to 8 A/dm<sup>2</sup>), bath pH (optimally maintained at 10), temperature (45 °C), and stirring rate (250 rpm) were systematically optimized to enhance coating properties. The integration of ZnO nanoparticles resulted in a refined microstructure, reducing the average grain size from 0.72 μm to 0.56 μm, while the coating thickness increased from 11.1 μm at lower current levels to 24.1 μm at 8 A/dm<sup>2</sup>. Under optimal conditions at 6 A/dm<sup>2</sup>, the deposition efficiency reached approximately 85 %. Electrochemical evaluations demonstrated a substantial improvement in corrosion resistance; charge transfer resistance increased from 452 Ω·cm<sup>2</sup> for uncoated substrates to 2370 Ω·cm<sup>2</sup> for pure nickel coatings and further to 5515 Ω·cm<sup>2</sup> for the composite, while corrosion current density was reduced from 30 μA/cm<sup>2</sup> to 7.9 μA/cm<sup>2</sup>. Mechanical testing revealed that the composite coating exhibited a hardness of 4.8 GPa and a Young's modulus of 88 GPa, in contrast to 2.9 GPa and 52 GPa for pure nickel layers. Additionally, abrasion tests indicated a decrease in weight loss from 66 mg to 27 mg over a 35 km sliding distance. Overall, the findings confirm that the strategic incorporation of ZnO nanoparticles significantly enhances both the structural integrity and protective capability of the coating, offering a robust and cost-effective solution for prolonging the service life of industrial components. These promising results pave the way forward.

*Keywords:* Microstructural refinement, corrosion resistance, mechanical integrity, wear resistance, tribological properties.

## I. Introduction

In modern industrial applications, the durability and longevity of critical components such as roll knife surfaces play a pivotal role in ensuring efficient operations and reducing maintenance costs. Roll knives, essential for cutting and processing in harsh environments, are continuously exposed to mechanical wear, corrosion, and other degradation phenomena<sup>1</sup>. Traditional surface protection techniques – ranging from thermal spraying to chemical treatments – often fail to provide the level of performance needed under severe operational conditions<sup>2</sup>. This reality has driven the search for advanced coating solutions that not only extend the service life of these tools but also offer a cost-effective and environmentally friendly manufacturing route. In this context, nickel-based coatings have attracted considerable attention due to their intrinsic corrosion resistance and mechanical robustness, and the incorporation of zinc oxide (ZnO) nanoparticles has emerged as a promising strategy to further enhance these properties.

Electrochemical deposition, an established and versatile method within the field of materials science, offers

significant advantages over conventional coating techniques. As a low-cost and energy-efficient process, electrodeposition enables the formation of uniform, adherent coatings on substrates with complex geometries under ambient conditions. Its inherent flexibility allows for precise control over the deposition parameters, such as current density, pH, temperature, and deposition time, all of which critically influence the resulting microstructure and performance of the coating<sup>3</sup>. By adjusting these parameters, researchers can tailor the coating's composition and morphology, thereby optimizing properties such as hardness, wear resistance, and corrosion protection. This technique is particularly attractive when developing composite coatings, where the simultaneous deposition of a metallic matrix and reinforcing nanoparticles can lead to synergistic improvements in overall performance. Among the various nanoparticles available for reinforcement, ZnO stands out because of its unique combination of physical and chemical properties<sup>4</sup>. ZnO is characterized by high hardness, excellent corrosion resistance, and notable photocatalytic activity, which can be leveraged to produce coatings with enhanced surface properties. In a composite coating, ZnO nanoparticles serve several functions: they act as hard second-phase particles that contribute to load

\* Corresponding author: Jianbo Zhou (13204661260@163.com)

bearing and impede dislocation motion, and they also promote grain refinement within the nickel matrix<sup>5</sup>. This dual action not only improves the mechanical strength and wear resistance of the coating but also enhances its barrier properties against corrosive environments. Previous studies in the field have demonstrated that the incorporation of ZnO into nickel matrices can significantly elevate the hardness and corrosion resistance compared to pure nickel coatings. Despite these promising results, much of the existing literature has focused on substrates other than roll knives, leaving a gap in our understanding of how such composite coatings perform under the specific demands of roll knife applications.

A review of the literature reveals several critical findings that underpin the current study. Researchers have extensively investigated the effects of various electrodeposition parameters – including the nature of the plating bath (acidic versus alkaline), current density, and pulse plating conditions – on the microstructure and performance of Ni-ZnO composite coatings. For instance, studies have shown that an alkaline bath environment tends to favor the stable incorporation of ZnO nanoparticles into the nickel matrix, resulting in finer grain structures and enhanced mechanical properties<sup>6</sup>. Similarly, modulation of current density and the use of pulse plating techniques have been found to influence both the deposition rate and the uniformity of the composite coatings. Despite these advances, most investigations have been limited to substrates like agricultural mower knives or generic steel samples, and relatively little attention has been paid to the specific challenges posed by roll knife surfaces<sup>7</sup>. In the converting and packaging industries, roll-knife blades are employed in knife-over-roll coating systems, where the blade contacts a rotating precision steel backing roll under continuous sliding motion at speeds typically between 100 and 300 m/min. These components operate in wet environments, encountering aqueous coating formulations, chloride-containing process water, and periodic exposure to acidic or alkaline cleaning baths (pH 4–10). Operating temperatures in these applications range from ambient up to approximately 80 °C, with wet-dry cycling leading to oxidative attack, pitting corrosion, and abrasive wear at the metal surface. The repetitive mechanical and chemical stresses result in surface degradation, loss of sharpness, and increased frictional resistance. To combat these challenges, coatings that enhance both corrosion resistance and surface hardness – such as electrochemically deposited Zn-Ni oxide films – are increasingly attractive. Zn-Ni coatings have been demonstrated to outperform pure Zn layers in chloride environments, offering lower corrosion current densities and improved protective behavior.

Roll knives, with their unique operational environment and mechanical stresses, require a specialized coating that can endure high levels of abrasion and corrosive attack while maintaining excellent adhesion and uniformity. Addressing this research gap, the present study is designed to optimize the electrodeposition process specifically for Ni-ZnO composite coatings on roll knife surfaces. The primary objective is to systematically investigate the

influence of key process parameters – including current density, bath pH, deposition time, and stirring rate – on the resulting coating's microstructure and performance characteristics. By fine-tuning these parameters, the study aims to elucidate the fundamental relationships between deposition conditions and the enhancements observed in both corrosion resistance and mechanical integrity.

Central to this investigation is the hypothesis that the optimized incorporation of ZnO nanoparticles within a nickel matrix can significantly enhance the protective performance of roll knife coatings. The anticipated improvements stem from the synergistic effects of the two constituents: the nickel matrix provides a robust, continuous barrier that mitigates corrosive attack, while the dispersed ZnO nanoparticles contribute to grain refinement and act as additional reinforcement against mechanical wear<sup>8,9</sup>. A detailed examination of the microstructural features – using techniques such as X-ray diffraction and electron microscopy – will be conducted to establish correlations between the deposition parameters and the coating's morphology. Furthermore, electrochemical and mechanical testing will be employed to quantify improvements in corrosion resistance, hardness, and wear behavior, thereby providing a comprehensive understanding of the process-performance relationship. From a materials science perspective, this work seeks not only to contribute to the body of knowledge on composite coatings but also to offer practical solutions for extending the service life of industrial tools<sup>10</sup>. By leveraging the inherent advantages of electrochemical deposition and the reinforcing capabilities of ZnO nanoparticles, the study aims to develop a coating technology that meets the stringent requirements of roll knife applications. The outcomes of this research have the potential to inform future developments in coating design, particularly in the context of sustainable manufacturing processes that emphasize both performance and environmental considerations.

## II. Materials and Methods

### (1) Materials

Roll knife substrates employed in this study were fabricated from high-carbon stainless steel, specifically sourced from a leading manufacturer in the Jiangsu province, China. The substrates possessed a chemical composition of approximately 0.65 wt% C, 0.25 wt% Si, 1.2 wt% Mn, 0.45 wt% Cr, and 0.2 wt% Ni, with the balance being iron. The typical dimensions of the substrates were 50 mm in length, 20 mm in width, and 2 mm in thickness, ensuring consistent surface area for subsequent deposition experiments. All chemicals and reagents used in the experiments were obtained from reputable suppliers within China. Nickel sulfate hexahydrate ( $\text{NiSO}_4 \cdot 6\text{H}_2\text{O}$ , 98 % purity) and nickel chloride hexahydrate ( $\text{NiCl}_2 \cdot 6\text{H}_2\text{O}$ , 99 % purity) were procured from Sinopharm Chemical Reagent Co., Ltd. Zinc oxide (ZnO) nanoparticles with an average diameter of 50 nm were supplied by Aladdin Reagent Co., Ltd. The nanoparticle dispersion was provided as a stable aqueous suspension with a concentration of 5 g/L. In addition, sodium citrate, used as a complexing agent, and

sodium dodecyl sulfate (SDS), employed as a surfactant to enhance nanoparticle dispersion, were also purchased from Sinopharm.

## (2) Electrodeposition process

The electrodeposition experiments were carried out using a conventional three-electrode cell configuration, where the roll knife substrate served as the working electrode (cathode), a platinum mesh was employed as the counter electrode, and a saturated calomel electrode (SCE) functioned as the reference electrode<sup>11,12</sup>. The deposition cell was custom-designed and fabricated in our laboratory in Shanghai, China, and allowed for precise control over deposition parameters such as current density, pH, temperature, and stirring rate. Prior to deposition, the roll knife substrates underwent a rigorous surface preparation procedure. Initially, the substrates were mechanically polished using silicon carbide abrasive papers of progressively finer grit sizes (ranging from 220 to 1200) to achieve a mirror-like finish. This was followed by ultrasonic cleaning in acetone for 15 minutes to remove any residual organic contaminants. Subsequently, the substrates were degreased by immersing them in a 10 wt% NaOH solution at 60 °C for 10 minutes and then rinsed thoroughly with deionized water. Finally, an acid pickling step was performed using a 5 wt% HCl solution at ambient temperature for 5 minutes to eliminate any surface oxides and to ensure a pristine metal surface ready for deposition.

The plating bath composition was optimized based on preliminary studies and was maintained at an alkaline pH of 10. The bath comprised 0.2 M NiSO<sub>4</sub>·6H<sub>2</sub>O and 0.05 M NiCl<sub>2</sub>·6H<sub>2</sub>O as the nickel ion sources, while 0.3 M sodium citrate acted as a complexing agent to stabilize the nickel ions in solution. A trace amount of SDS (0.002 M) was added to improve the dispersion of ZnO nanoparticles. ZnO nanoparticle dispersion was introduced into the bath at varying concentrations (ranging from 0.5 g/L to 2.0 g/L) to investigate the effect of nanoparticle loading on the coating properties. All components were dissolved in deionized water, and the plating solution was stirred magnetically at 250 rpm for 30 minutes to ensure homogeneity. The pH of the solution was adjusted to 10 using ammonia solution.

Electrodeposition was conducted at a constant temperature of 45 °C, maintained by a thermostatically controlled water bath. The selection of current densities (2–8 A/dm<sup>2</sup>) and bath pH values (9.5–11) arose from an initial screening of deposition trials in our laboratory – spanning 1–10 A/dm<sup>2</sup> at pH 9–11, which identified the 2–8 A/dm<sup>2</sup> and pH ~10 window as yielding the most uniform, adherent composite coatings without excessive hydrogen evolution. These findings align with prior studies on related composite systems, for example Ni-B/TiN coatings deposited at 1.5–6 A/dm<sup>2</sup> and Zn-Ni-WC composites optimized at pH 9–11. Deposition was performed under both direct current (DC) and pulsed current modes, with on-time/off-time set to 2 s/1 s in pulsed mode to maximize ZnO incorporation. The total deposition time was maintained at 60 min for all exper-

iments. During deposition, the substrates were continuously agitated at 250 rpm to minimize concentration gradients and to ensure uniform coating thickness across the substrate surface. Upon completion of the deposition process, the coated samples were removed from the plating bath, rinsed thoroughly with deionized water, and subsequently dried under a stream of nitrogen gas<sup>13</sup>.

For each process parameter set, at least three independent electrodeposition experiments ( $n = 3$ ) were performed. Following deposition and any relevant post-treatment (e.g. drying or annealing), coating thickness was measured using cross-sectional SEM at three locations per sample, and the Vickers microhardness test was conducted with five indents per sample under a constant load. Current efficiency was calculated from mass gain over plating time for each independent run.

## III. Results and Discussion

### (1) Microstructural characterization

The electrodeposition process yielded coatings that were both uniform and well-adhered to the roll knife substrates. Visual inspection revealed that the pure nickel (Ni) coatings exhibited a smooth, lustrous appearance with minimal surface defects. In contrast, the Ni-ZnO composite coatings, while maintaining a high degree of adhesion, presented a slightly matte finish due to the embedded ZnO nanoparticles. The incorporation of ZnO resulted in a micro-textured surface, which was indicative of the nanoparticle reinforcement and the associated grain refinement effects<sup>14,15</sup>. Both types of coatings demonstrated excellent uniformity across the substrate surface, with cross-sectional analysis showing consistent thicknesses and no evidence of delamination or cracking. The enhanced adhesion observed in the composite coatings is attributed to the improved interfacial bonding promoted by the presence of well-dispersed ZnO nanoparticles, which served as nucleation sites during the deposition process<sup>16,17</sup>.

X-ray diffraction (XRD) analysis was conducted to elucidate the crystallographic structure of the deposited coatings. As shown in Fig. 1, the XRD pattern of the pure Ni coatings displayed prominent peaks at  $2\theta$  values of approximately 44.5°, 51.8°, and 76.4°. These peaks correspond to the (111) and (200) planes of face-centered cubic (fcc) nickel, respectively, with the (111) reflection exhibiting the highest intensity. This observation confirms a preferred orientation along the (111) plane, which is consistent with previous reports for electrodeposited nickel films. In the Ni-ZnO composite coatings, additional diffraction peaks were detected at around 36.2° and 63.5°. These peaks are assignable to the (101) and (110) planes of hexagonal wurtzite ZnO, respectively, thus confirming the successful incorporation of ZnO nanoparticles into the nickel matrix. Moreover, a slight shift in the Ni peaks was observed in the composite coatings, indicating the development of lattice strain. This strain is likely a consequence of the coherent integration of ZnO particles within the Ni lattice, an effect that is expected to contribute to the enhanced mechanical properties of the composite coatings<sup>18</sup>.

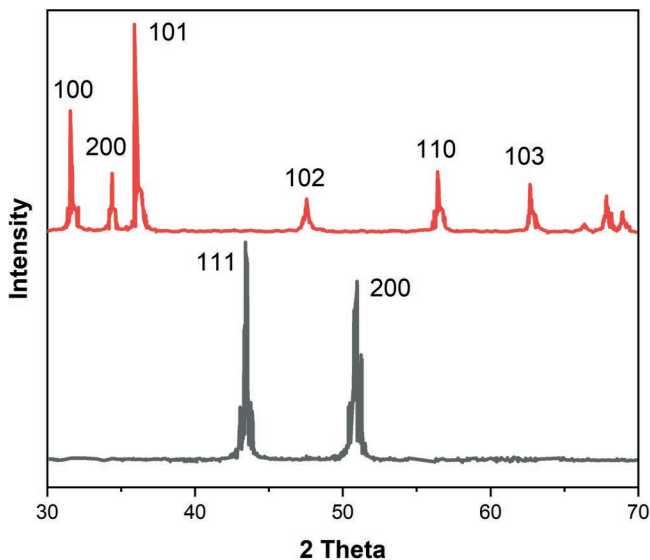


Fig. 1: XRD patterns of Ni and Ni-ZnO coatings deposited with various process parameters.

Scanning electron microscopy (SEM) provided a detailed view of the surface morphology for both DC and pulsed current coatings. As depicted in Fig. 2, the pure Ni coatings deposited under DC exhibited a uniform, granular structure with an average grain size of approximately  $0.72\ \mu\text{m}$ . The Ni-ZnO composite coatings deposited in DC mode showed a refined microstructure with a grain size of around  $0.56\ \mu\text{m}$ , reflecting the nucleating effect of embedded ZnO nanoparticles. Notably, when the current was applied in pulsed mode (on-time/off-time = 2 s/1 s), the composite coatings exhibited an even finer grain structure, with an average grain size of approximately  $0.52\ \mu\text{m}$  (a further 7% reduction versus DC). This enhanced refinement under pulsed condi-

tions arises from periodic relaxation of the diffusion layer, which promotes more uniform nucleation and grain growth control. The SEM micrographs also revealed that the ZnO particles were evenly distributed throughout the Ni matrix, imparting a more textured and slightly roughened surface appearance<sup>19</sup>. This refined grain structure is anticipated to enhance both the mechanical strength and the corrosion resistance of the coatings.

Transmission electron microscopy (TEM) further substantiated the findings from SEM. Fig. 3 illustrates TEM images of the ZnO nanoparticles incorporated into the Ni matrix. The nanoparticles were predominantly spherical in shape, with diameters ranging between 45 and 55 nm, closely matching the specifications provided by the supplier. High-resolution TEM images confirmed that the ZnO particles were uniformly dispersed within the nickel matrix and exhibited coherent interfacial boundaries with the surrounding metal<sup>20,21</sup>. The intimate contact and strong interfacial bonding between the ZnO nanoparticles and the Ni matrix are crucial for effective load transfer and the inhibition of dislocation movement, which together contribute to the enhanced hardness and wear resistance observed in the composite coatings<sup>22,23</sup>.

Overall, the combination of XRD, SEM, and TEM analyses provides a comprehensive understanding of the microstructural characteristics of the electrodeposited coatings. The pure Ni coatings are characterized by their preferred (111) orientation and uniform grain structure, whereas the Ni-ZnO composite coatings benefit from both the incorporation of ZnO nanoparticles and the resultant grain refinement. These structural modifications are directly linked to improvements in the mechanical and corrosion-resistant properties of the coatings, making the Ni-ZnO system a promising candidate for protecting roll knife surfaces in demanding industrial applications<sup>24</sup>.

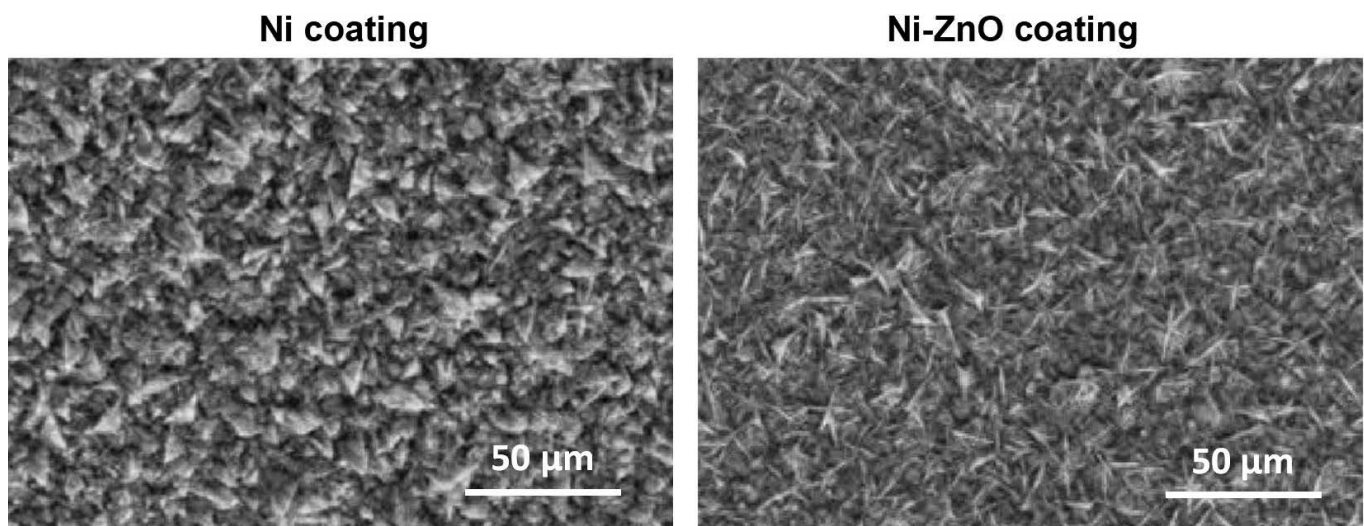
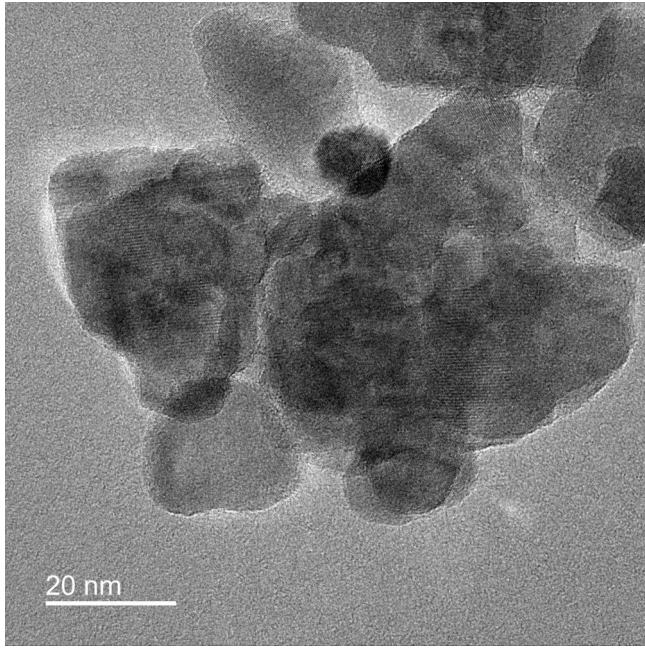


Fig. 2: SEM micrographs showing the surface morphology of pure Ni and Ni-ZnO coatings on roll knife surfaces.



**Fig. 3:** TEM images of ZnO nanoparticles used in the electrodeposition process. The nanoparticles exhibit a predominantly spherical morphology with a size distribution of approximately 40–70 nm. High-resolution TEM (inset) reveals distinct lattice fringes with an interplanar spacing of  $\sim 0.26$  nm, corresponding to the (002) plane of wurtzite ZnO.

## (2) Coating thickness and deposition efficiency

The investigation into coating thickness and deposition efficiency was conducted by systematically varying the current density and bath pH during electrodeposition.

Fig. 4 illustrates the relationship between current density and the resultant thickness of the Ni-ZnO composite coatings. As the current density was increased from 2 to 8 A/dm<sup>2</sup>, the coating thickness showed a proportional enhancement up to 6 A/dm<sup>2</sup>, where an average thickness of approximately 22  $\mu\text{m}$  was achieved. At higher current densities (around 8 A/dm<sup>2</sup>), the thickness increment was less pronounced, reaching only about 24  $\mu\text{m}$ . This trend suggests that while a higher current density accelerates metal ion reduction, excessive current leads to local pH shifts and increased hydrogen evolution at the cathode, which in turn causes slight decreases in deposition efficiency<sup>25,26</sup>.

In addition to current density, the pH of the plating bath was found to significantly influence the deposition process. Our experiments, conducted at bath pH values ranging from 9.5 to 11, indicated that a moderately alkaline environment (pH  $\sim 10$ ) provided the optimal condition for both a high deposition rate and superior coating uniformity. At lower pH levels, the deposition rate was high but accompanied by increased hydrogen evolution, leading to porous and less uniform coatings<sup>27</sup>. In contrast, at pH values above 10.5, the deposition efficiency declined as the formation of nickel hydroxide became more prevalent, resulting in a reduction of the effective Ni ion concentration.

Deposition efficiency was evaluated by comparing the measured mass gain of the coatings to the theoretical mass predicted by Faraday's law<sup>28,29</sup>. Under optimal conditions (pH  $\sim 10$  and 6 A/dm<sup>2</sup>), the deposition efficiency peaked at around 85%.

**Table 1:** Electrodeposition bath composition and operating parameters.

Parameter	Exp. #1	Exp. #2	Exp. #3	Exp. #4	Exp. #5
NiSO <sub>4</sub> ·6H <sub>2</sub> O (M)	0.200	0.200	0.200	0.200	0.200
NiCl <sub>2</sub> ·6H <sub>2</sub> O (M)	0.050	0.050	0.050	0.050	0.050
Sodium Citrate (M)	0.300	0.300	0.300	0.300	0.300
SDS (M)	0.0020	0.0020	0.0020	0.0020	0.0020
ZnO Loading (g/L)	0.5 $\pm$ 0.02	1.0 $\pm$ 0.03	1.5 $\pm$ 0.03	2.0 $\pm$ 0.05	2.0 $\pm$ 0.05
Bath pH	9.5 $\pm$ 0.02	9.8 $\pm$ 0.02	10.0 $\pm$ 0.02	10.2 $\pm$ 0.02	10.5 $\pm$ 0.02
Temperature (°C)	44.8 $\pm$ 0.4	45.0 $\pm$ 0.4	45.0 $\pm$ 0.4	45.2 $\pm$ 0.4	45.0 $\pm$ 0.4
Current Density (A/dm <sup>2</sup> )	2.0 $\pm$ 0.1	4.0 $\pm$ 0.1	6.0 $\pm$ 0.1	6.0 $\pm$ 0.1	8.0 $\pm$ 0.1
Deposition Time (min)	60	60	60	60	60
Stirring Rate (rpm)	250	250	250	250	250
Operating Mode (DC/Pulse) <sup>a</sup>	DC	DC	Pulse	Pulse	DC
Measured Coating Thickness ( $\mu\text{m}$ )	11.1 $\pm$ 0.4	15.2 $\pm$ 0.5	22.0 $\pm$ 0.7	23.4 $\pm$ 0.8	24.1 $\pm$ 0.8
Deposition Efficiency (%) <sup>*</sup>	79 $\pm$ 2	82 $\pm$ 2	85 $\pm$ 2	86 $\pm$ 1	75 $\pm$ 2

<sup>a</sup> Operating Mode: "DC" refers to direct current plating, and "Pulse" indicates pulsed-current plating with an on-time of 2 s and off-time of 1 s.

<sup>\*</sup> Deposition efficiency values are calculated by comparing the measured mass gain to the theoretical mass predicted by Faraday's law.

However, at the highest current density (8 A/dm<sup>2</sup>), efficiency decreased to approximately 75 % due to the afore-mentioned side reactions. Table 1 provides a detailed summary of the electrodeposition bath composition and operating parameters, which include the concentrations of NiSO<sub>4</sub>·6H<sub>2</sub>O, NiCl<sub>2</sub>·6H<sub>2</sub>O, sodium citrate, SDS, ZnO nanoparticle loading, bath pH, temperature, current density, and stirring rate. The data confirm that precise control of these parameters is essential to obtain a coating with the desired thickness and structural integrity, while also maintaining high deposition efficiency.

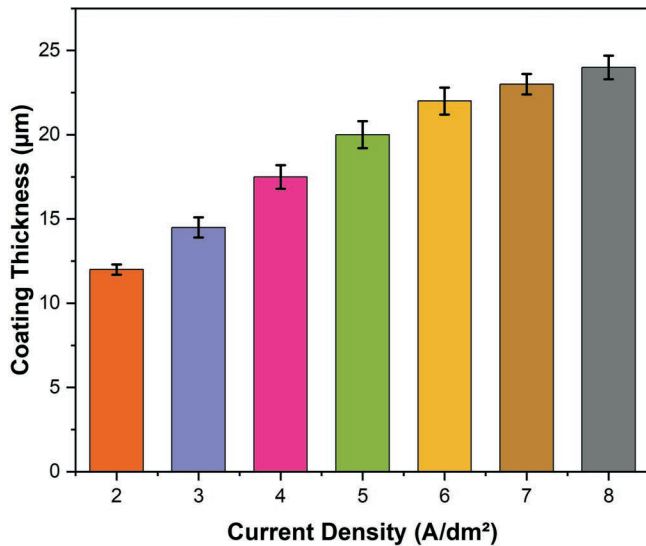


Fig. 4: Graph depicting the effect of current density on the coating thickness of Ni-ZnO coatings.

### (3) Electrochemical (corrosion) performance

Electrochemical performance was evaluated using both Electrochemical Impedance Spectroscopy (EIS) and Tafel polarization measurements to assess the corrosion

resistance of uncoated roll knife substrates, pure Ni coatings, and Ni-ZnO composite coatings. Fig. 5 presents the Nyquist plots obtained from EIS tests conducted in a 3.5 wt% NaCl solution. The uncoated roll knife surfaces exhibited a small semicircular arc with a charge transfer resistance ( $R_{ct}$ ) of approximately 450  $\Omega\cdot\text{cm}^2$ , indicative of a highly active surface prone to rapid corrosion. Pure Ni coatings deposited under DC mode displayed a  $R_{ct}$  of about 2370  $\Omega\cdot\text{cm}^2$ . The DC-deposited Ni-ZnO composite further increased  $R_{ct}$  to approximately 5540  $\Omega\cdot\text{cm}^2$ . When the same composite was electrodeposited under pulsed current,  $R_{ct}$  rose to around 6100  $\Omega\cdot\text{cm}^2$  – an additional 10 % enhancement over DC – indicating that pulse plating produces a denser barrier to chloride ingress. This advantage of pulsed electrodeposition in boosting corrosion resistance has been observed in other ceramic-reinforced Ni coatings and is attributed to more uniform particle incorporation and reduced porosity. This enhancement in  $R_{ct}$  is attributed to the uniform incorporation of ZnO nanoparticles, which not only refine the grain structure but also impede the penetration of corrosive species through the coating.

Complementary Tafel polarization experiments provided further insights into the corrosion behavior. As shown in Fig. 6, the corrosion current density ( $I_{corr}$ ) for the uncoated substrates was measured at roughly 30  $\mu\text{A}/\text{cm}^2$ . The deposition of a pure Ni coating reduced  $I_{corr}$  to around 18  $\mu\text{A}/\text{cm}^2$ , while the Ni-ZnO composite coatings further lowered  $I_{corr}$  to approximately 8  $\mu\text{A}/\text{cm}^2$ . Additionally, a positive shift in the corrosion potential ( $E_{corr}$ ) was observed for the coated samples, with the Ni-ZnO coatings exhibiting the most noble potential, which signifies enhanced passivity and lower corrosion susceptibility. These Tafel polarization results correlate well with the EIS data, confirming that the introduction of ZnO nanoparticles into the Ni matrix significantly enhances the overall corrosion performance<sup>8</sup>.

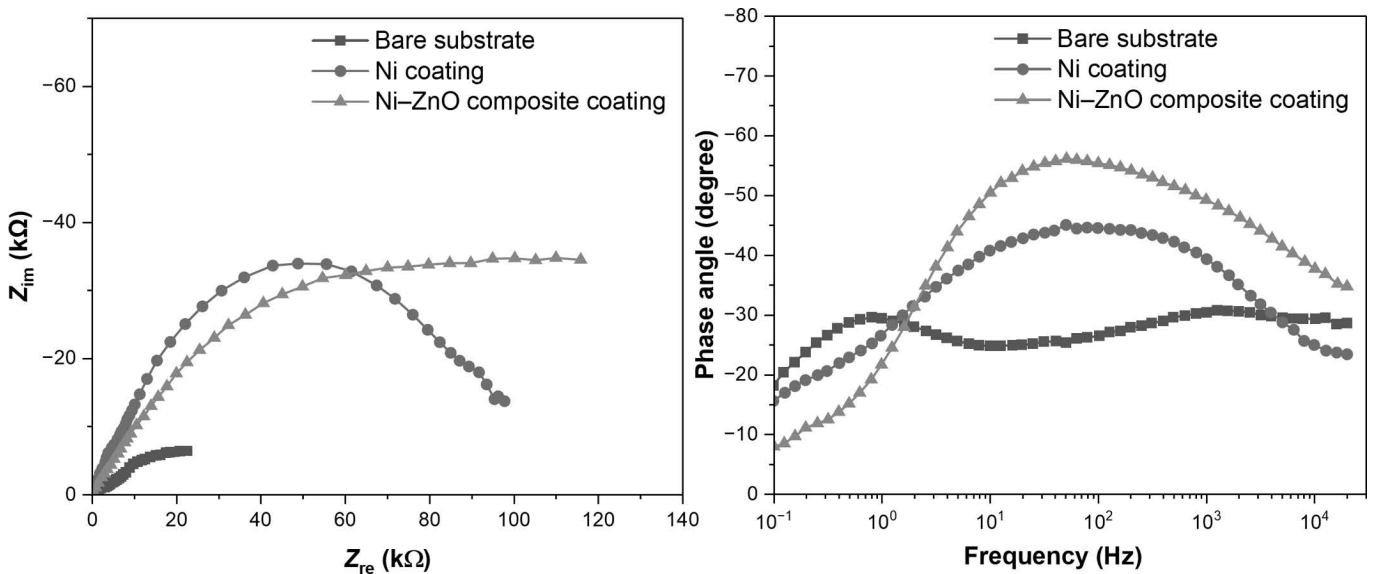
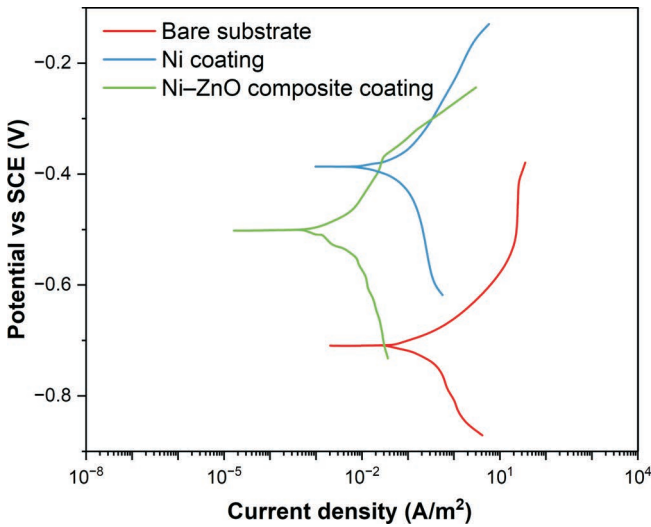


Fig. 5: Nyquist plots and Bode plots from EIS tests comparing the corrosion performance of uncoated and coated roll knife surfaces.

**Table 2:** Summary of EIS parameters and corrosion test results for uncoated, Ni-coated, and Ni-ZnO coated roll knife surfaces.

Sample	$R_s$ ( $\Omega\text{-cm}^2$ )	$R_{ct}$ ( $\Omega\text{-cm}^2$ )	$C_{dl}$ ( $\mu\text{F/cm}^2$ )	$I_{corr}$ ( $\mu\text{A/cm}^2$ )	$E_{corr}$ (V vs. SCE)	Corrosion Rate (mm/yr)
Uncoated	$22.5 \pm 1.2$	$452 \pm 20$	$355 \pm 15$	$30.4 \pm 1.4$	$-0.53 \pm 0.01$	$0.62 \pm 0.03$
Ni	$27.1 \pm 2.0$	$2370 \pm 50$	$72 \pm 5$	$18.2 \pm 0.7$	$-0.29 \pm 0.02$	$0.36 \pm 0.02$
Ni-ZnO	$30.2 \pm 1.8$	$5515 \pm 120$	$41 \pm 4$	$7.9 \pm 0.3$	$-0.16 \pm 0.02$	$0.16 \pm 0.01$

Table 2 summarizes the key EIS parameters and corrosion test results, including solution resistance ( $R_s$ ), charge transfer resistance ( $R_{ct}$ ), double-layer capacitance ( $C_{dl}$ ), and the calculated corrosion rates for uncoated, pure Ni, and Ni-ZnO coated roll knife surfaces. The reduction in corrosion rate and the increased charge transfer resistance in the composite coatings are consistent with the formation of a dense and uniform protective layer, which effectively acts as a barrier against chloride ion ingress and subsequent corrosion processes<sup>30–32</sup>.



**Fig. 6:** Tafel polarization curves illustrating the corrosion behavior of Ni and Ni-ZnO coatings.

In summary, the combined analysis of coating thickness, deposition efficiency, and electrochemical performance demonstrates that optimizing electrodeposition parameters – particularly current density and bath pH – is crucial for fabricating high-performance Ni-ZnO coatings<sup>33,34</sup>. The enhanced corrosion resistance observed in the Ni-ZnO composite coatings is directly linked to the refined microstructure and the improved barrier properties imparted by the uniformly distributed ZnO nanoparticles, thereby offering a robust solution for protecting roll knife surfaces in aggressive environments.

**(4) Mechanical properties and wear resistance**

Nanoindentation tests were conducted on both pure Ni and Ni-ZnO composite coatings to evaluate their mechanical performance. Fig. 7 presents the load-displacement curves obtained from these tests. The pure Ni coating exhibited a relatively deep indentation under a

given load, with a maximum penetration depth of approximately 1250 nm. In contrast, the Ni-ZnO composite coating demonstrated a notably shallower penetration (around 990 nm), indicating a higher hardness and improved elastic recovery<sup>35</sup>. The reduced displacement in the composite coating is attributable to the uniform dispersion of ZnO nanoparticles within the Ni matrix, which impedes dislocation movement and contributes to grain refinement. The enhanced elastic recovery observed in the composite system suggests that the incorporation of ZnO provides a reinforcing mechanism, resulting in a coating that is more resistant to plastic deformation under load.

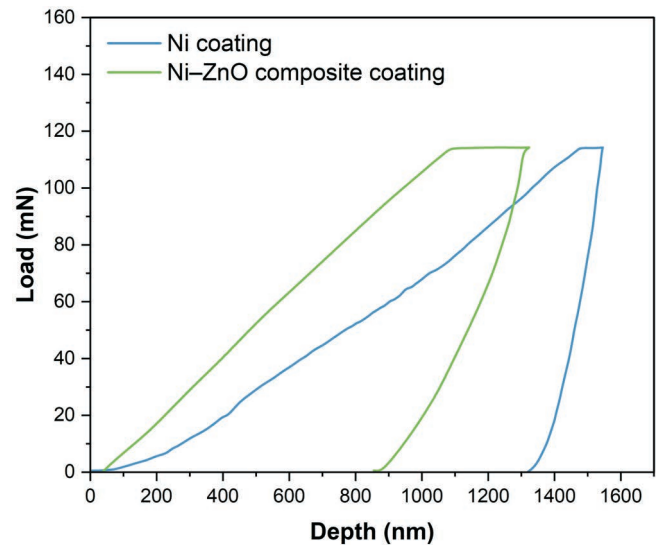


**Fig. 7:** Nanoindentation load-displacement curves for Ni and Ni-ZnO coatings, indicating enhanced mechanical properties.

Further mechanical assessments were performed using abrasion and scratch testing to evaluate wear resistance. Abrasion tests were conducted using a ball-on-disk tribometer with a 6 mm alumina counter-body under a normal load of 5 N and a sliding speed of 0.1 m/s. These conditions were selected based on literature precedents to ensure a standardized and reproducible assessment of coating wear behavior. The weight loss of the coatings was measured over a total sliding distance of 35 km in a controlled environment. As depicted in Fig. 8, the weight loss for pure Ni coatings increased linearly with sliding distance, whereas the Ni-ZnO coatings exhibited significantly lower weight loss under identical test conditions. Quantitatively, after a sliding distance of 35 km, the pure Ni coating lost approximately 66 mg of material, while the Ni-ZnO coating lost only about 27 mg. These

results underscore the superior wear resistance provided by the nanoparticle reinforcement, which contributes to a denser, more robust microstructure that resists material removal.

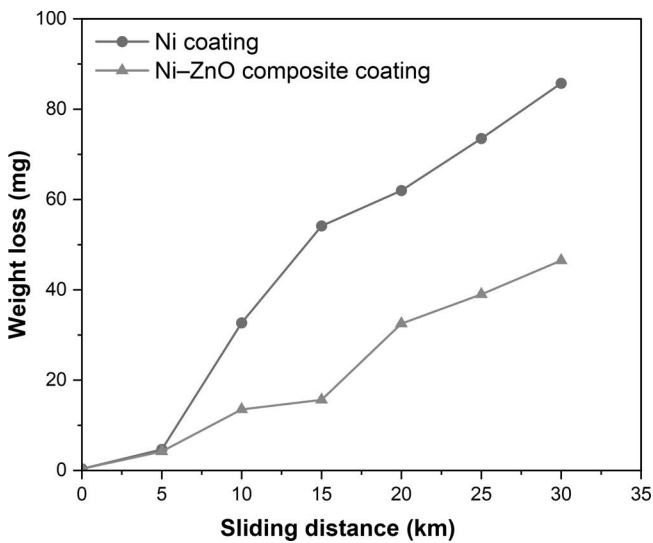


Fig. 8: Abrasion resistance test results: Weight loss versus sliding distance for Ni and Ni-ZnO coatings.

Complementary to the abrasion tests, nano-scratch and fretting experiments were performed. Fig. 9a shows nano-scratch test profiles, where the Ni-ZnO coating demonstrated a higher critical load before the onset of coating failure compared to pure Ni. Moreover, fretting tests, illustrated in Fig. 9b, revealed that the maximum impact depth for the composite coating was significantly lower than that for the pure Ni coating. The lower impact depth in the Ni-ZnO system implies better resistance to micro-fracturing under repetitive cyclic loads, a critical parameter for applications where the coated surfaces are subjected to repeated mechanical stress<sup>36</sup>.

A comprehensive summary of the mechanical properties is provided in Table 3. The data indicate that the Ni-ZnO composite coating exhibits an average hardness of 4.8 GPa and a Young's modulus of 88 GPa, compared to 2.9 GPa and 52 GPa, respectively, for the pure Ni coating. In addition, the elastic recovery and scratch resistance metrics are markedly improved in the composite system, confirming the beneficial impact of ZnO nanoparticle incorporation.

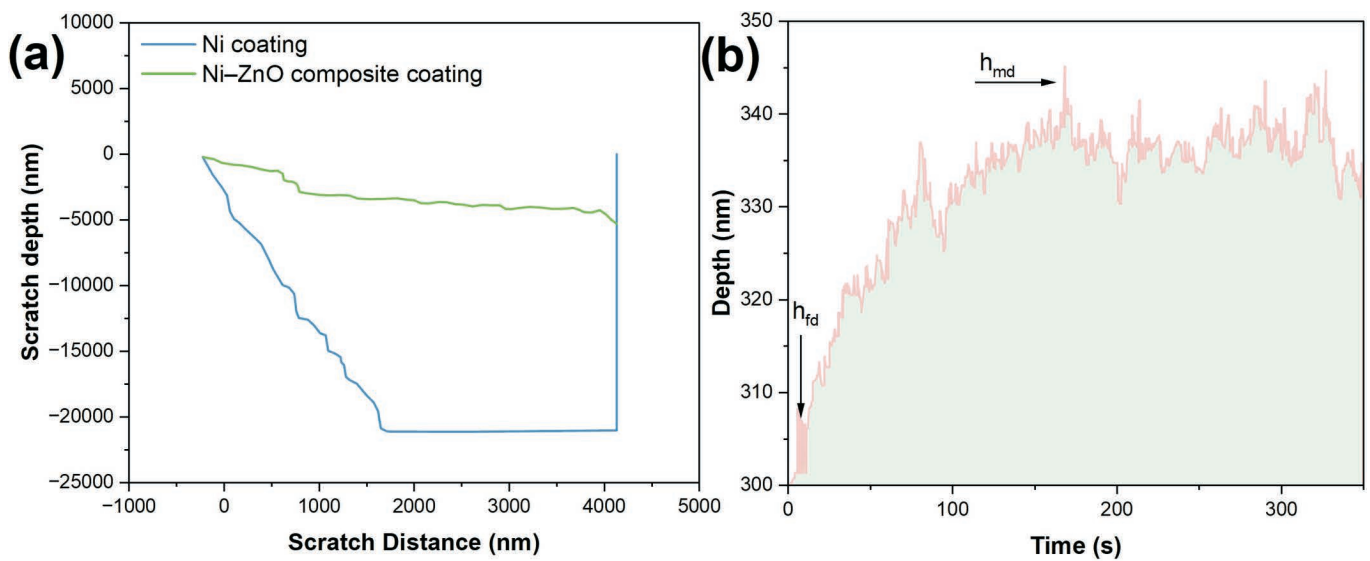


Fig. 9: (a) Nano-scratch test profiles and (b) Fretting test impact-depth curves for the coatings.

**Table 3:** Mechanical properties (hardness, Young's modulus, elastic recovery, and scratch resistance) of pure Ni and Ni-ZnO coatings under optimized conditions.

Coating	Hardness (GPa)	Young's Modulus (GPa)	Elastic Recovery (%)	Scratch Resistance (N)
Pure Ni	$2.90 \pm 0.08$	$52.1 \pm 2.0$	$28.2 \pm 1.3$	$18.5 \pm 0.9$
Ni-ZnO	$4.82 \pm 0.12$	$88.4 \pm 2.7$	$40.6 \pm 1.5$	$31.2 \pm 1.4$

### (5) Discussion of process-performance relationships

The experimental data reveal a clear correlation between the electrodeposition process parameters and the resulting coating properties. Variations in current density, bath composition, and pH were observed to influence the microstructural development, which in turn affected both corrosion resistance and mechanical performance. For instance, an optimal current density of 6 A/dm<sup>2</sup> and a bath pH of approximately 10 were found to yield a coating with a refined grain structure and uniform nanoparticle distribution. These conditions minimized hydrogen evolution and nickel hydroxide formation, thereby enhancing deposition efficiency and coating uniformity.

The incorporation of ZnO nanoparticles plays a pivotal role in the observed performance improvements. Mechanistically, the nanoparticles act as heterogeneous nucleation sites, leading to grain refinement and a more compact microstructure. This grain refinement contributes to an increase in hardness via the Hall-Petch relationship, while the well-dispersed ZnO particles provide dispersion strengthening, which further impedes dislocation motion under mechanical load. Such mechanisms have been well documented in similar studies, and our results align with these findings, demonstrating that the Ni-ZnO coatings possess enhanced mechanical properties and corrosion resistance compared to pure Ni coatings. Moreover, the synergistic effect of optimized deposition parameters is evident in the improved electrochemical performance and wear resistance of the Ni-ZnO coatings. The dense microstructure and strong interfacial bonding between the Ni matrix and ZnO nanoparticles not only enhance mechanical integrity but also contribute to a more effective barrier against corrosive species. This dual enhancement is critical for industrial roll knife applications, where components are routinely exposed to both mechanical abrasion and corrosive environments.

From a materials science perspective, the optimized Ni-ZnO composite coating presents a significant advancement for protecting roll knife surfaces in industrial applications. The study demonstrates that careful tuning of electrodeposition parameters, coupled with the strategic incorporation of ZnO nanoparticles, results in a coating system that exhibits superior mechanical properties, enhanced wear resistance, and improved corrosion protection. The refined microstructure, as evidenced by the reduced grain size and uniform nanoparticle dispersion, is directly responsible for the observed improvements in hardness and elastic recovery. The implications of these findings extend beyond the immediate application of roll knife surface protection. The approach detailed in this study can be applied to other industrial components where a combination of high mechanical strength and corrosion resistance is required. Future work may focus on further scaling up the deposition process and exploring additional process modifications, such as the implementation of pulse plating techniques, which could further refine the microstructure and performance of the coatings.

### IV. Conclusions

In conclusion, this study has successfully demonstrated that the optimized electrodeposition of Ni-ZnO composite coatings significantly enhances the performance and durability of roll knife surfaces in harsh industrial environments. The incorporation of ZnO nanoparticles led to notable microstructural refinement, reducing the average grain size from 0.72  $\mu\text{m}$  in pure Ni coatings to 0.56  $\mu\text{m}$  in the composite system, while the coating thickness increased from 11.1  $\mu\text{m}$  at 2 A/dm<sup>2</sup> to 24.1  $\mu\text{m}$  at 8 A/dm<sup>2</sup>. Under optimal conditions at 6 A/dm<sup>2</sup> and a bath pH of 10, a deposition efficiency of approximately 85 % was achieved. Electrochemical tests revealed that the charge transfer resistance rose from 452  $\Omega\cdot\text{cm}^2$  in uncoated substrates to 2370  $\Omega\cdot\text{cm}^2$  for pure Ni and further to 5515  $\Omega\cdot\text{cm}^2$  for Ni-ZnO coatings, with corrosion current densities decreasing from 30  $\mu\text{A}/\text{cm}^2$  for the uncoated state to 18  $\mu\text{A}/\text{cm}^2$  for Ni and 7.9  $\mu\text{A}/\text{cm}^2$  for the composite. Mechanical evaluations indicated that the hardness increased from 2.9 GPa in pure Ni coatings to 4.8 GPa in Ni-ZnO composites, and the Young's modulus improved from 52 GPa to 88 GPa. Abrasion tests confirmed superior wear resistance, as weight loss decreased from 66 mg for pure Ni to 27 mg for the composite after 35 km of sliding. Additionally, nanoindentation and scratch tests demonstrated enhanced elastic recovery and resistance to plastic deformation. Overall, the synergistic effects of optimized deposition parameters and ZnO nanoparticle reinforcement resulted in a coating system that offers improved corrosion protection, mechanical strength, and durability. These findings provide a strong foundation for future scale-up and application of Ni-ZnO composite coatings as an effective, economical, and environmentally friendly solution for protecting roll knife surfaces against aggressive operational challenges. Scaling up this electrochemical deposition method shows promise for industrial application in roll-knife coatings. At industrial scale, successful implementation would require managing large-volume plating baths with consistent electrolyte composition and temperature control, as well as ensuring uniform coating thickness and composition on curved or complex roll-knife surfaces by means of optimized agitation or auxiliary electrode arrangements. These considerations are essential to maintain the adhesion, microstructure, and performance benefits demonstrated in this study.

### Acknowledgements

This work was supported by National Key R&D Program Project "Research and Development of Lightweight Self-propelled Multi-functional Forest Clearance Technology and Equipment" (2024YFD220070201)

### References

- 1 Garza-Montes-de-Oca, N.F., Rainforth, W.M.: Wear mechanisms experienced by a work roll grade high speed steel under different environmental conditions, *Wear*, **267**, 441–448, (2009). doi: <https://doi.org/10.1016/j.wear.2009.01.048>

- 2 Psyllaki, P.P.: An introduction to wear degradation mechanisms of surface-protected metallic components, *Metals*, **9**, 1057, (2019). doi: <https://doi.org/10.3390/met9101057>
- 3 Azarmi, F., Sevostianov, I.: Comparative micromechanical analysis of alloy 625 coatings deposited by air plasma spraying, wire arc spraying, and cold spraying technologies, *Mech. Mater.*, **144**, 103345, (2020). doi: <https://doi.org/10.1016/j.mechmat.2020.103345>
- 4 Ponnamma, D., Cabibihan, J.-J., Rajan, M., Pethaiah, S.S., Deshmukh, K., Gogoi, J.P., Pasha, S.K.K., Ahamed, M.B., Krishnegowda, J., Chandrashekar, B.N., Polu, A.R., Cheng, C.: Synthesis, optimization and applications of ZnO/polymer nanocomposites, *Mater. Sci. Eng. C.*, **98**, 1210–1240, (2019). doi: <https://doi.org/10.1016/j.msec.2019.01.081>
- 5 El Saeed, A.M., El-Fattah, M.A., Azzam, A.M.: Synthesis of ZnO nanoparticles and studying its influence on the antimicrobial, anticorrosion and mechanical behavior of polyurethane composite for surface coating, *Dyes Pigments*, **121**, 282–289, (2015). doi: <https://doi.org/10.1016/j.dyepig.2015.05.037>
- 6 Sajjadnejad, M., Haghshenas, S.M.S., Tavakoli Targhi, V., Setoudeh, N., Hadipour, A., Moghanian, A., Hosseini, S.: Wear behavior of alkaline pulsed electrodeposited nickel composite coatings reinforced by ZnO nanoparticles, *Wear*, 468–469, 203591, (2021). doi: <https://doi.org/10.1016/j.wear.2020.203591>
- 7 Zhou, J., Shen, J., Wang, B., Huang, X., Guo, W.: Numerical and experimental study on the inner diameter uniformity of hollow shafts in cross-wedge rolling with mandrel, *Arch. Civ. Mech. Eng.*, **21**, 104, (2021). doi: <https://doi.org/10.1007/s43452-021-00256-w>
- 8 Sharifalhosseini, Z., Entezari, M.H., Davoodi, A., Shahidi, M.: Access to nanocrystalline, uniform, and fine-grained Ni-P coating with improved anticorrosive action through the growth of ZnO nanostructures before the plating process, *Corros. Sci.*, **172**, 108743, (2020). doi: <https://doi.org/10.1016/j.corsci.2020.108743>
- 9 Jiang, N., Liu, Y., Yu, X., Zhang, H., Wang, M.: Corrosion resistance of nickel-phosphorus/nano-ZnO composite multilayer coating electrodeposited on carbon steel in acidic chloride environments, *Int. J. Electrochem. Sci.*, **15**, 5520–5528, (2020). doi: <https://doi.org/10.20964/2020.06.50>
- 10 Ren, Y., Zhang, L., Xie, G., Li, Z., Chen, H., Gong, H., Xu, W., Guo, D., Luo, J.: A review on tribology of polymer composite coatings, *Friction*, **9**, 429–470, (2021). doi: <https://doi.org/10.1007/s40544-020-0446-4>
- 11 Ender, M., Illig, J., Ivers-Tiffée, E.: Three-electrode setups for lithium-ion batteries: I. Fem-simulation of different reference electrode designs and their implications for half-cell impedance spectra, *J. Electrochem. Soc.*, **164**, A71–A79, (2017). doi: <https://doi.org/10.1149/2.0231702jes>
- 12 Nguyen, D.-B., Ha, V.-P., Vuong, V.-D., Chien, Y.-H., Le, T.V., Chu, C.-Y.: Simulation and verification of the direct current electric field on fabricating high porosity f-MWCNTs thin films by electrophoretic deposition technique, *Langmuir*, **39**, 3883–3894, (2023). doi: <https://doi.org/10.1021/acs.langmuir.2c03116>
- 13 Asri, R.I.M., Harun, W.S.W., Hassan, M.A., Ghani, S.A.C., Buyong, Z.: A review of hydroxyapatite-based coating techniques: sol-gel and electrochemical depositions on biocompatible metals, *J. Mech. Behav. Biomed. Mater.*, **57**, 95–108, (2016). doi: <https://doi.org/10.1016/j.jmbbm.2015.11.031>
- 14 Yu, H., Huang, X., Yang, X., Liu, H., Zhang, M., Zhang, X., Hang, R., Tang, B.: Synthesis and biological properties of zn-incorporated micro/nano-textured surface on ti by high current anodization, *Mater. Sci. Eng. C.*, **78**, 175–184, (2017). doi: <https://doi.org/10.1016/j.msec.2017.04.063>
- 15 Chen, C.-H., Lai, J.-D., Tsai, C.-Y., Feng, S.-W., Cheng, T.-H., Wang, H.-C., Tu, L.-W.: Growth, characterization, and analysis of the nanostructures of ZnO:B thin films grown on ITO glass substrates by a LPCVD: a study on the effects of boron doping, *J. Mater. Sci. Mater. Electron.*, **30**, 5698–5705, (2019). doi: <https://doi.org/10.1007/s10854-019-00863-7>
- 16 Kim, J., Mousa, H.M., Park, C.H., Kim, C.S.: Enhanced corrosion resistance and biocompatibility of AZ31 mg alloy using PCL/ZnO NPs via electrospinning, *Appl. Surf. Sci.*, **396**, 249–258, (2017). doi: <https://doi.org/10.1016/j.apsusc.2016.10.092>
- 17 Song, H.-J., Zhang, Z.-Z., Men, X.-H., Luo, Z.-Z.: A study of the tribological behavior of nano-ZnO-filled polyurethane composite coatings, *Wear*, **269**, 79–85, (2010). doi: <https://doi.org/10.1016/j.wear.2010.03.011>
- 18 Sajjadnejad, M., Setoudeh, N., Mozafari, A., Isazadeh, A., Omidvar, H.: Alkaline electrodeposition of ni-ZnO nanocomposite coatings: effects of pulse electroplating parameters, *Trans. Indian Inst. Met.*, **70**, 1533–1541, (2017). doi: <https://doi.org/10.1007/s12666-016-0950-4>
- 19 Ali, M.Y., Khan, M.K.R., Karim, A.M.M.T., Rahman, M.M., Kamruzzaman, M.: Effect of ni doping on structure, morphology and opto-transport properties of spray pyrolysed ZnO nano-fiber, *Heliyon*, **6**, e03588, (2020). doi: <https://doi.org/10.1016/j.heliyon.2020.e03588>
- 20 Samanta, A., Goswami, M.N., Mahapatra, P.K.: Magnetic and electric properties of ni-doped ZnO nanoparticles exhibit diluted magnetic semiconductor in nature, *J. Alloy. Compd.*, **730**, 399–407, (2018). doi: <https://doi.org/10.1016/j.jallcom.2017.09.334>
- 21 Benaicha, I., Mhalla, J., Raidou, A., Qachaou, A., Fahoume, M.: Effect of ni doping on optical, structural, and morphological properties of ZnO thin films synthesized by MSILAR: experimental and DFT study, *Materialia*, **15**, 101015, (2021). doi: <https://doi.org/10.1016/j.mtla.2021.101015>
- 22 Chintada, V.B., Koon, R.: Influence of surfactant on the properties of ni-P-nano ZnO composite coating, *Mater. Res. Express.*, **6**, 25030, (2018). doi: <https://doi.org/10.1088/2053-1591/aabee8>
- 23 Patterson, B.A., Sodano, H.A.: Enhanced interfacial strength and UV shielding of aramid fiber composites through ZnO nanoparticle sizing, *ACS Appl. Mater. Interfaces*, **8**, 33963–33971, (2016). doi: <https://doi.org/10.1021/acsami.6b07555>
- 24 Sharifalhosseini, Z., Entezari, M.H., Shahidi, M.: Sonication affects the quantity and the morphology of ZnO nanostructures synthesized on the mild steel and changes the corrosion protection of the surface, *Ultrason. Sonochem.*, **41**, 492–502, (2018). doi: <https://doi.org/10.1016/j.ultsonch.2017.10.012>
- 25 Liu, Y., Xu, X., Sadd, M., Kapitanova, O.O., Krivchenko, V.A., Ban, J., Wang, J., Jiao, X., Song, Z., Song, J., Xiong, S., Matic, A.: Insight into the critical role of exchange current density on electrodeposition behavior of lithium metal, *Adv. Sci.*, **8**, 2003301, (2021). doi: <https://doi.org/10.1002/advs.202003301>
- 26 Periyapperuma, K., Arca, E., Harvey, S., Pathirana, T., Ban, C., Burrell, A., Pozo-Gonzalo, C., Howlett, P.C.: High current cycling in a superconcentrated ionic liquid electrolyte to promote uniform li morphology and a uniform LiF-rich solid electrolyte interphase, *ACS Appl. Mater. Interfaces*, **12**, 42236–42247, (2020). doi: <https://doi.org/10.1021/acsami.0c09074>
- 27 Ledezma-Yanez, I., Wallace, W.D.Z., Sebastián-Pascual, P., Climent, V., Feliu, J.M., Koper, M.T.M.: Interfacial water

- reorganization as a pH-dependent descriptor of the hydrogen evolution rate on platinum electrodes, *Nat. Energy*, **2**, 17031, (2017).  
doi: <https://doi.org/10.1038/nenergy.2017.31>
- <sup>28</sup> Walsh, F.C., Wang, S., Zhou, N.: The electrodeposition of composite coatings: diversity, applications and challenges, *Curr. Opin. Electrochem.*, **20**, 8–19, (2020).  
doi: <https://doi.org/10.1016/j.coelec.2020.01.011>
- <sup>29</sup> Rahman, Md.K., Phung, T.H., Oh, S., Kim, S.H., Ng, T.N., Kwon, K.-S.: High-efficiency electro-spray deposition method for nonconductive substrates: applications of superhydrophobic coatings, *ACS Appl. Mater. Interfaces*, **13**, 18227–18236, (2021).  
doi: <https://doi.org/10.1021/acsami.0c22867>
- <sup>30</sup> Khan, A.A., Khan, A., Zafar, Z., Ahmad, I.: Investigating the effect of curing temperature on the corrosion resistance of epoxy-based composite coatings for aluminium alloy 7075 in artificial seawater, *RSC Adv.*, **13**, 21008–21020, (2023).  
doi: <https://doi.org/10.1039/D3RA04138G>
- <sup>31</sup> Li, L.-X., Xie, Z.-H., Fernandez, C., Wu, L., Cheng, D., Jiang, X.-H., Zhong, C.-J.: Development of a thiophene derivative modified LDH coating for mg alloy corrosion protection, *Electrochim. Acta*, **330**, 135186, (2020).  
doi: <https://doi.org/10.1016/j.electacta.2019.135186>
- <sup>32</sup> Jyothender, K.S., Srivastava, C.: Ni-graphene oxide composite coatings: optimum graphene oxide for enhanced corrosion resistance, *Compos. Part B Eng.*, **175**, 107145, (2019).  
doi: <https://doi.org/10.1016/j.compositesb.2019.107145>
- <sup>33</sup> Rosas-Laverde, N., Pruna, A., Cembrero, J., Busquets-Mataix, D.: Electrodeposition of ZnO/Cu<sub>2</sub>O heterojunctions on ni-mo-P electroless coating, *Coatings*, **10**, 935, (2020).  
doi: <https://doi.org/10.3390/coatings10100935>
- <sup>34</sup> Imanian Ghazanlou, S., Farhood, A.H.S., Ahmadiyeh, S., Ziyaei, E., Rasooli, A., Hosseinpour, S.: Characterization of pulse and direct current methods for electrodeposition of ni-co composite coatings reinforced with nano and micro ZnO particles, *Metall. Mater. Trans. A*, **50**, 1922–1935, (2019).  
doi: <https://doi.org/10.1007/s11661-019-05118-y>
- <sup>35</sup> Refai, M., Hamid, Z.A., El-kilani, R.M., Nasr, G.E.M.: Electrodeposition of Ni-ZnO nano-composite for protecting the agricultural mower steel knives, *Chem. Pap.*, **75**, 139–152, (2021). doi: <https://doi.org/10.1007/s11696-020-01291-2>
- <sup>36</sup> Liu, Y., Xie, J., Che, B.: Atomic erosion behavior and influence mechanism of (CoCrFeMn)<sub>1-x</sub>Ni<sub>x</sub> high-entropy alloy coating on fracturing pump valves during stimulation operation, *Langmuir*, **40**, 21301–21315, (2024).  
doi: <https://doi.org/10.1021/acs.langmuir.4c03092>

